DOI: 10.14529/jsfi240308

Numerical Analysis of OECD/NEA HYMERES Project Benchmark Tests Using CABARET-SC1 CFD Code

Anton A. Kanaev[1]***, Vyacheslav Yu. Glotov***[1]

The benchmark tests carried out within the OECD/NEA HYMERES (HYdrogen Mitigation Experiments for Reactor Safety) international project allowed to assess the capability of computational tools and to develop methodology for improving the modelling of complex safety issues relevant for the analysis and mitigation of a severe accident leading to hydrogen release into a nuclear plant containment. The paper presents the results of numerical simulation of two OECD/NEA HYMERES benchmark tests using CABARET-SC1 code. The code is based on the eddy resolving CABARET technique, which allows implicit modeling of the subgrid turbulence scales without using tuning parameters (ILES approximation). The absence of tuning parameters in the numerical approach allowed evaluating the influence of a separate physical phenomenon of radiative heat transfer. The influence of the mesh resolution in flow regions with complex geometries and the use of a porous medium model was also investigated.

Keywords: CFD modeling, NPP hydrogen safety, ILES.

Introduction

During a severe accident at a nuclear power plant (NPP) with water-cooled reactors, a significant amount of hydrogen can be produced due to the oxidation of the zirconium cladding of the fuel rods at high temperatures. The release of hydrogen into the containment volume can lead to the formation of explosive mixtures of hydrogen and air, the combustion and detonation of which pose a serious threat to the integrity of the containment. During the Three Mile Island NPP accident in 1979, about 350 kg of hydrogen burned, fortunately causing no damage to the containment and thus not leading to significant radiological consequences for the environment or the population [3]. In more recent instance, during the Fukushima Daiichi NPP accident [6], a series of hydrogen explosions occurred, damaging the reactor buildings and resulting in the release of radioactivity into the atmosphere.

The distribution of hydrogen in the containment and the potential for the formation of localized areas with high hydrogen concentration are determined by complex thermal and hydraulic processes occurring at different stages of a severe accident. Therefore, ensuring the hydrogen explosion safety of NPPs during severe accidents represents a complex scientific and technical problem. Its solution requires a comprehensive approach, including both analytical and experimental research.

The first (2013–2016) [9] and second (2017–2021) [10] phases of the international OECD/NEA HYMERES project included experimental studies on the large-scale PANDA facility (PSI, Switzerland). The project aimed to improve understanding of thermal-hydraulic processes in severe accident scenarios involving hydrogen release into NPP containment, with an emphasis on the potential for mixing the areas of increased hydrogen concentration. Helium was used in all experiments to simulate hydrogen. All experiments were accompanied by analytical studies.

At the Nuclear Safety Institute (IBRAE), a non-parametric approach based on the CABARET method [1] is being developed for modeling turbulent flows in multicomponent media. CABARET belongs to eddy-resolving schemes with implicit subgrid turbulence modeling (ILES). It allows to carry out computations using meshes that do not fully resolve turbulence scales without using

[1]Nuclear Safety Institute (IBRAE), Moscow, Russian Federation

tuning parameters. The only source of uncertainties is the mesh resolution, the selection criterion of which is based on the analysis of solution convergence. The CABARET methodology forms the basis of the CFD code CABARET-SC1 hydrodynamic solver [4, 7].

Within each phase of the OECD/NEA HYMERES project, one of the experiments investigating the mixing process of a helium-rich region by a flow formed after the interaction of a vertical steam jet with an obstacle was chosen as a benchmark test. This paper contains two main sections devoted to the description of the experimental setup, the approaches used in modeling and the results of the numerical analysis of the benchmark tests from the first (HP1_6_2 test) and second (H2P1_10 test) phases of the OECD/NEA HYMERES project using CABARET-SC1 CFD code.

1. HP1_6_2 Test

One of the experiments on the PANDA facility with a horizontal obstacle shaped as a flat disk on the path of a vertical steam jet (HP1_6_2 test) was chosen as the benchmark test for the first phase of the OECD/NEA HYMERES project.

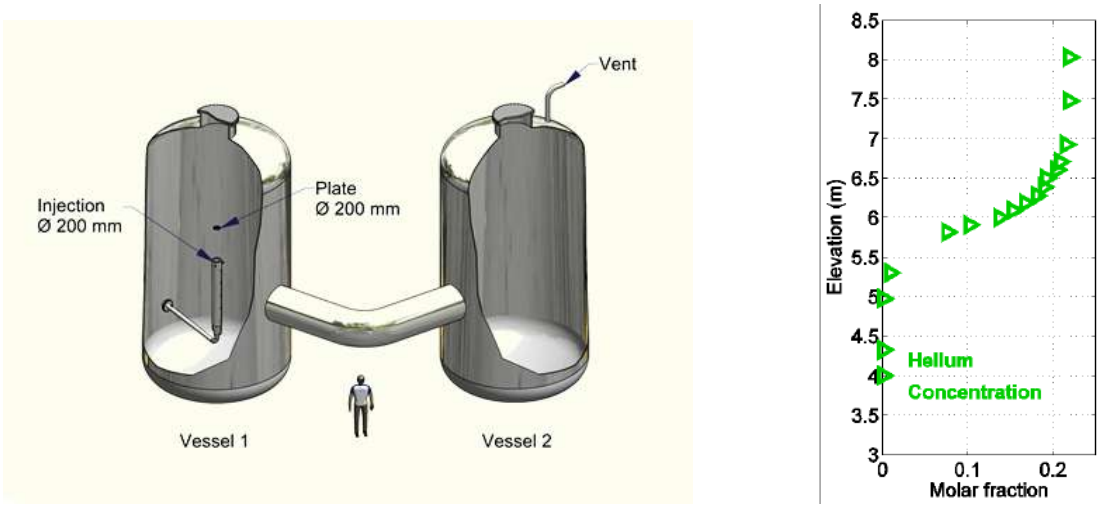

(a) Configuration of the PANDA facility in HP1_6_2 test

(b) Initial vertical profile of helium concentration in Vessel 1

Figure 1. HP1_6_2 test setup

The configuration of the PANDA facility in HP1_6_2 test is shown in Fig. 1a. The height of the volumes (vessels) of the facility is ~ 8 m, the diameter of each vessel is 4 m. Vessels are connected by a large (1 m) diameter Interconnecting Pipe (IP). During the pre-conditioning phase the vessels were filled with steam at 108°C and a helium-rich layer was created in the upper part of Vessel 1 (Fig. 1b). During the experiment, steam is injected from a round pipe located on the axis of Vessel 1. The outlet of the pipe is 2 m below the lower boundary of the helium-rich layer (which starts at 6 m from the bottom of Vessel 1). The steam flow rate is 60 g/s at a temperature of 150°C. Mixing is slowed down by a circular plate with a diameter of 20 cm, also located on the axis of the vessel at a distance of 1 m from the steam jet outlet. The pressure in the vessels during the experiment is maintained constant at 1.3 bar by venting the medium to the atmosphere through a valve at the top of Vessel 2. Before the start of the experiment,

the walls of the vessels (as well as the obstacle plate) were heated to the target temperature, ensuring the absence of condensation on the walls during the transient process.

During the experiment, the distribution of thermal-hydraulic variables in the volume of the experimental setup is measured using the PANDA instrumentation consisting in a variety of sensor types. To measure the temperature in Vessels 1 and 2 and in the connecting pipeline, 374 thermocouples were installed. Helium, steam, and air concentrations at the PANDA facility are measured using two mass spectrometers. The gas mixture was sampled through capillaries (139 in total) which were installed near the thermocouple locations. The distribution of concentration and temperature measurement points was chosen to obtain detailed information about the flow structures and the erosion of the helium-rich layer. Helium concentration was measured at six levels above the steam injection level.

To carry out the simulation two computational meshes were constructed: coarse ($\sim$ 1 million hexahedral cells) and refined in the area of the steam jet propagation and in the area of the obstacle ($\sim$ 3 million hexahedral cells).

The initial conditions were set as the approximation of the experimental measurements [11]. Thermal insulation of the PANDA facility was not modeled directly. A third-kind boundary condition $q = h \cdot (T - T_{ref})$ with a heat transfer coefficient obtained from the ad hoc heat loss measurements [12] $h = 5.77 \cdot 10^{-3} \cdot (T[K] - 1.66)$ was set on the external boundaries of the steel walls of the Vessels and the IP, with a reference temperature $T_{ref} = 20°\mathrm{C}$.

The computation of 1000 seconds of HP1_6_2 test on the Lomonosov-2 supercomputer [13] using CABARET-SC1 in the coarse mesh took about a week on 560 processors, and in the refined mesh – about two weeks on 980 processors. The time required for calculation is proportional not only to the overall number of cells but also to the numerical time steps which are reduced for the refined mesh in accordance with the CFL limitation.

Figure 2 shows a comparison of the vertical velocity distribution in experiment HP1_6_2 in the coarse and in the refined meshes. Different flow patterns of the steam jet in the area of the circular obstacle were observed. This is due to insufficient expansion of the modeled jet before the obstacle in the coarse mesh caused by insufficient resolution of the vortex flows formed in the mixing layer. In the refined mesh, the jet expands better and "reassembles"after the obstacle.

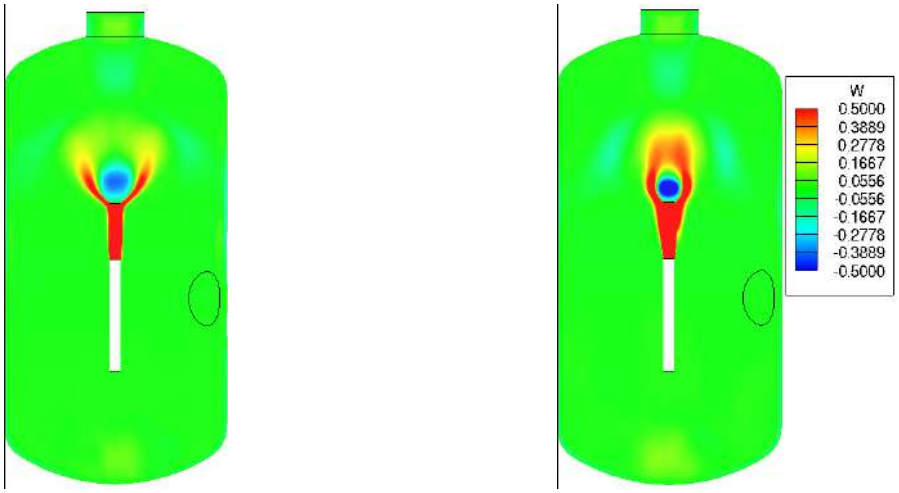

(a) Coarse mesh (b) Refined mesh

Figure 2. Distribution of the time-averaged vertical velocity in the calculations

Figure 3 shows the evolution of helium volume concentration and temperature at the point located on the axis of Vessel 1 at 2926 mm above the steam injection level for two meshes. It can be seen that the calculated helium concentration on the refined grid is significantly closer to the experimental measurements. Further calculations were conducted using the refined mesh.

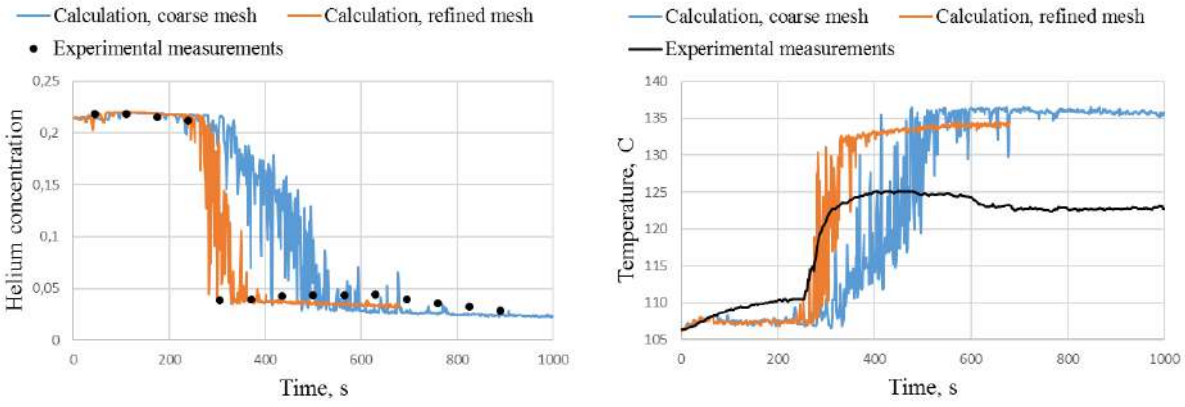

(a) (b)

Figure 3. Comparison of the calculated evolution of helium concentration (a) and temperature (b) with the experimental measurements

At the same time, it can be seen from Fig. 3b that the temperature is overestimated in the calculations for both meshes. One of the significant outcomes of the first phase of the OECD/NEA HYMERES project's benchmark test was the understanding that in tests with high steam content on the PANDA facility the heat transfer by radiation from the heated gas medium to the internal surface of the walls plays a significant role [12]. Experiments on the PANDA facility are conducted at relatively low steam temperatures ($\sim$ 100–150°C), but even at these temperatures, radiation is significant [5]. Estimates show that the medium is optically dense, so diffusion approximations can be used as a radiation model, in particular, the Rosseland model.

Inclusion of the Rosseland radiation heat transfer model in the calculation of HP1_6_2 test not only led to a good match between the calculated temperature and measurement results but also to a better approximation of the experimental helium concentration evolution in the upper area of Vessel 1. Due to more efficient heat removal by radiation from the gas medium to the walls in the calculation with the included Rosseland model, the vertical velocity of the steam flow after the obstacle is higher than in the calculation without considering radiation heat transfer due to its increased buoyancy (see Fig. 4).

The dynamics of the helium-enriched layer dissolution can be assessed by the decrease in helium concentration and the increase in temperature at sensors located on the axis of Vessel 1 at different heights above the steam injection level. Figures 5–7 show a comparison of helium concentration and temperature evolution in the calculation with the experimental measurements in the upper area of Vessel 1.

Observed differences in the time of the helium layer erosion at the two upper levels may be associated with increased heat losses in the area of the Vessel 1 manhole noted by the experimenters. These losses can be taken into account in the modeling using the measurements obtained with the wall thermocouples.

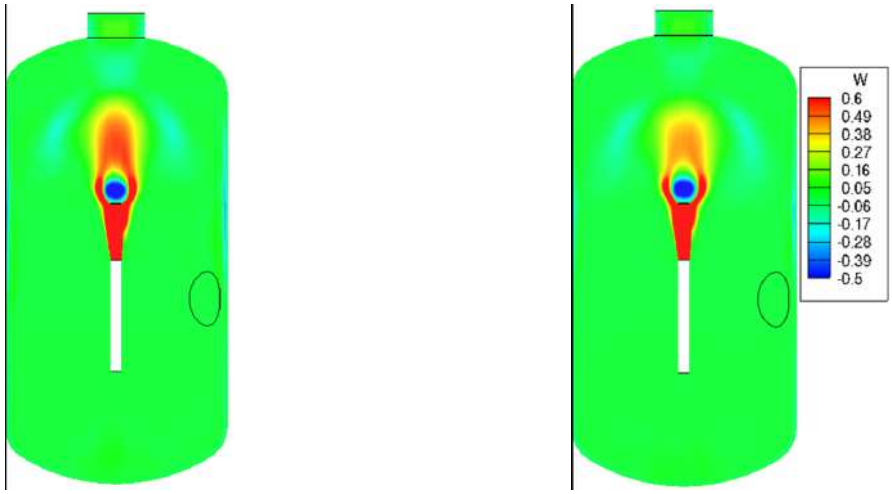

(a) Radiation heat transfer model included (b) No radiation heat transfer model

Figure 4. Distribution of the time-averaged vertical velocity in the calculations

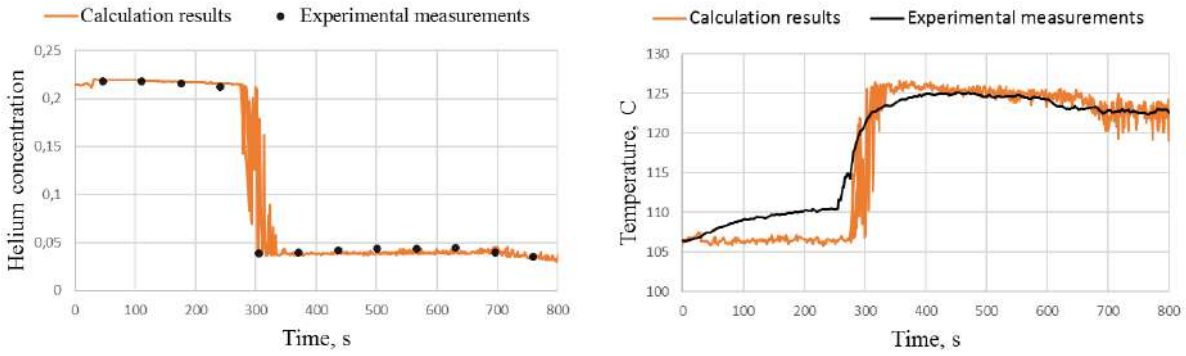

(a) (b)

Figure 5. Comparison of the evolution of calculated helium concentration (a) and temperature (b) with the experimental measurements at 2926 mm above the steam injection level

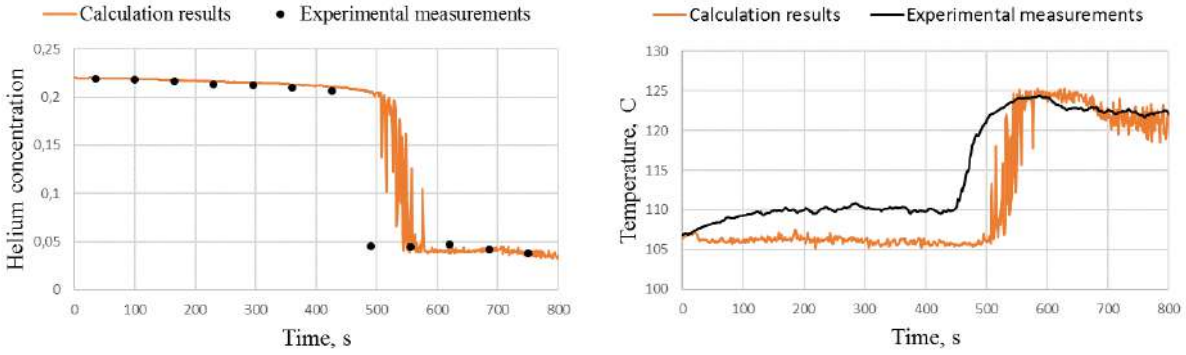

(a) (b)

Figure 6. Comparison of the evolution of calculated helium concentration (a) and temperature (b) with the experimental measurements at 3478 mm above the steam injection level

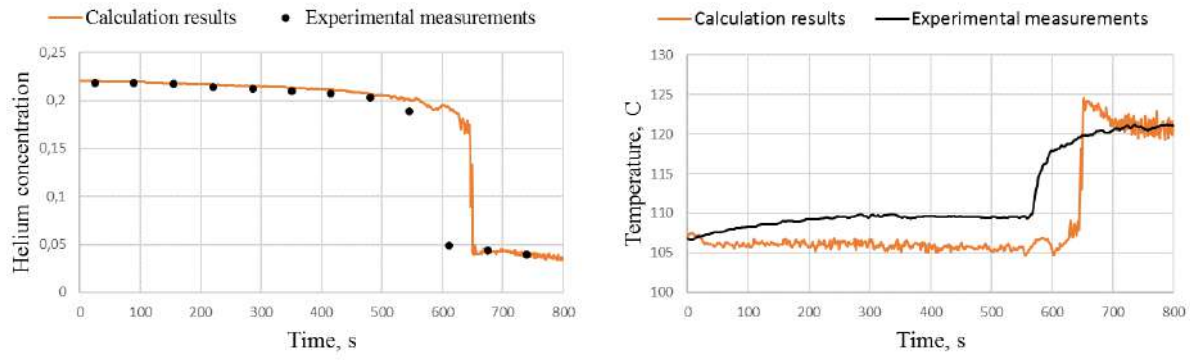

(a) (b)

Figure 7. Comparison of the evolution of calculated helium concentration (a) and temperature (b) with the experimental measurements at 4030 mm above the steam injection level

2. H2P1_10 Test

As a benchmark test for the second phase of the OECD/NEA HYMERES project experiment H2P1_10 was selected. The setup of H2P1_10 test differs from that of HP1_6_2 by the type of the obstacle in the path of the steam jet, which is a metal grid inclined at an angle of 17°C to the horizontal direction (Fig. 8a). The center of the grid is located at the height of 1.138 meters above the steam injection pipe. Unlike the first phase of the project, all experiments of the second phase were conducted in a single vessel of the PANDA facility (Vessel 1). The pressure during the experiments was relieved through a valve located at the bottom of Vessel 1.

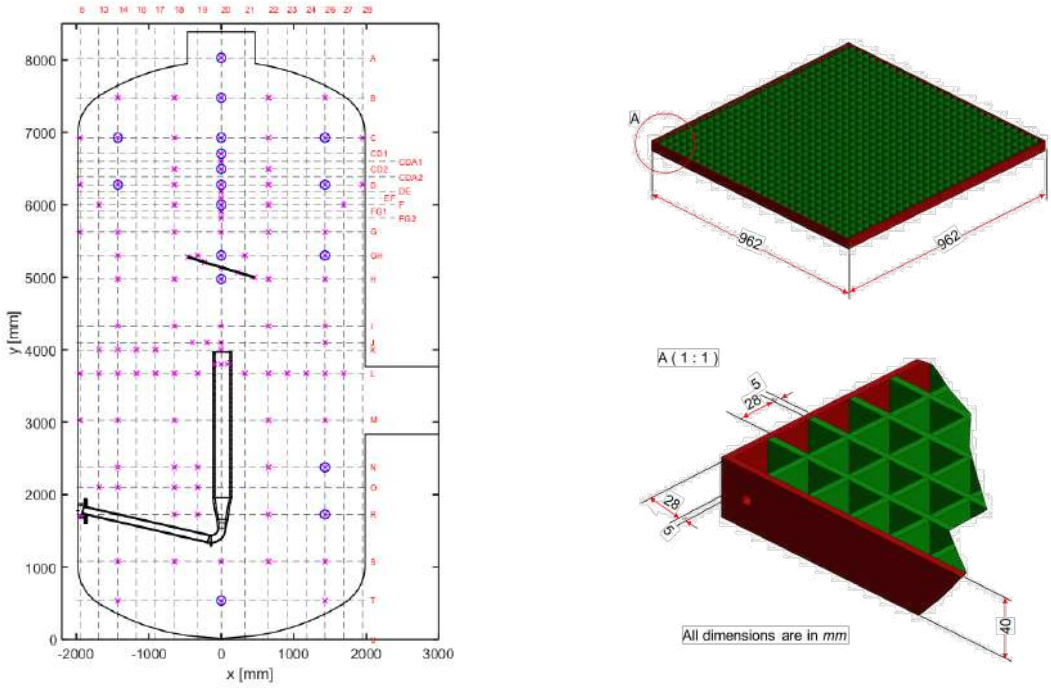

(a) Configuration of the PANDA experimental facility and the location of temperature and concentration measurement systems

(b) Geometrical characteristics of the inclined grid

Figure 8. H2P1_10 test setup

A complete simulation of the H2P1_10 test was carried out using a porous medium model (PMM) simulating the grid's resistance to the jet flow. The parameters of the PMM were adjusted using the averaged results of a detailed calculation of 40–70 seconds time interval with the direct mesh resolution of the steam flowing through the grid. For the reference detailed calculation of H2P1_10 test, a mesh with a resolution of $3 \times 3 \times 4$ cells for each grid hole and 777 cells in the steam injection pipe outlet, totaling ~ 9 million cells was constructed.

The number of computational cells in the mesh where the flow through the grid is not directly resolved is significantly lower than in the detailed mesh. For the calculation using PMM, the coarse (~ 1.75 million hexahedral cells, $47 \times 47 \times 2$ cells in the porous model area, 133 cells in the steam injection pipe outlet) and the refined (~ 2.7 million hexahedral cells, $57 \times 57 \times 2$ cells in the porous model area, 209 cells in the steam injection pipe outlet) meshes were constructed (Fig. 9).

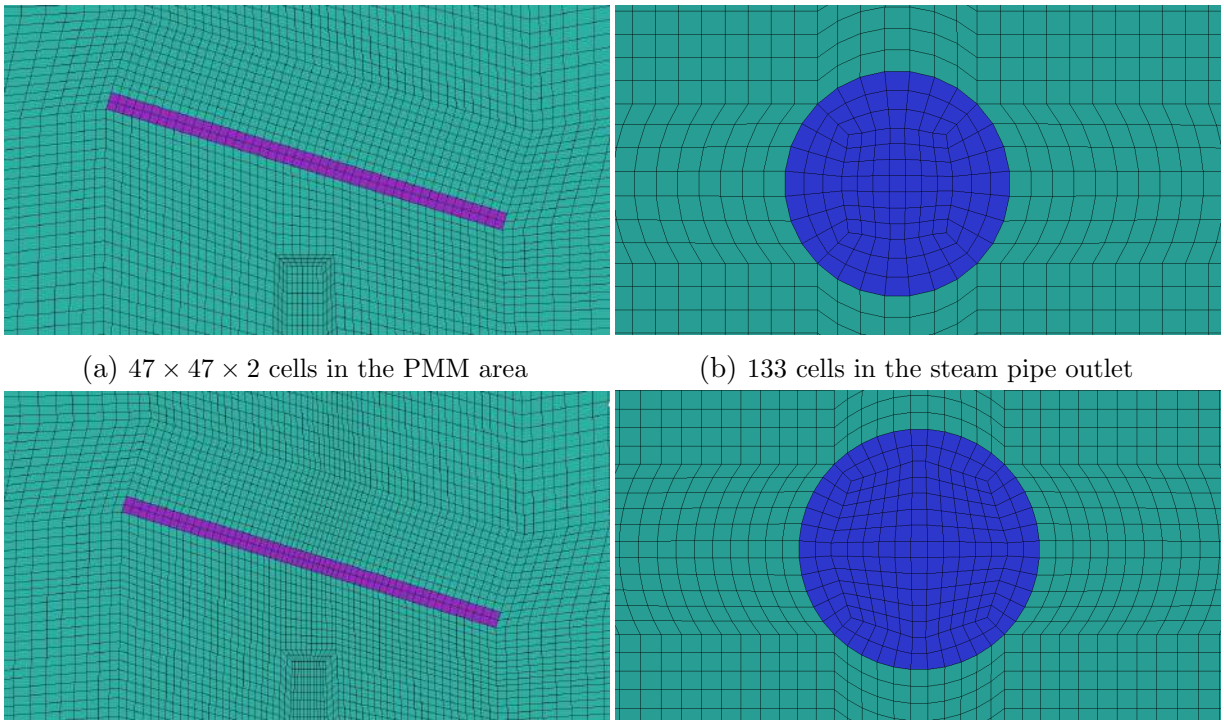

(a) $47 \times 47 \times 2$ cells in the PMM area

(b) 133 cells in the steam pipe outlet

(c) $57 \times 57 \times 2$ cells in the PMM area

(d) 209 cells in the steam pipe outlet

Figure 9. Comparison of the coarse (a, b) and the refined (c, d) meshes

The detailed calculation of the first 70 seconds of H2P1_10 test on the Lomonosov-2 supercomputer using CABARET-SC1 took about 70 hours on 1120 processors. The calculation using PMM in the refined mesh required approximately 6.7 times less core-hours than the detailed calculation.

Figure 10a shows the comparison of time-averaged velocity magnitude values in the jet along the horizontal line at an altitude of 5000 mm above the bottom point, just before the jet contacts the inclined grid (Fig. 10b) in the detailed calculation and in the calculations with PMM. The maximum velocity magnitude values in the detailed calculation and in the PMM calculation on the refined grid coincide, while in the PMM calculation on the coarse grid, due to insufficient resolution in the jet area, the peak velocity magnitude is overestimated by $\sim 8\%$.

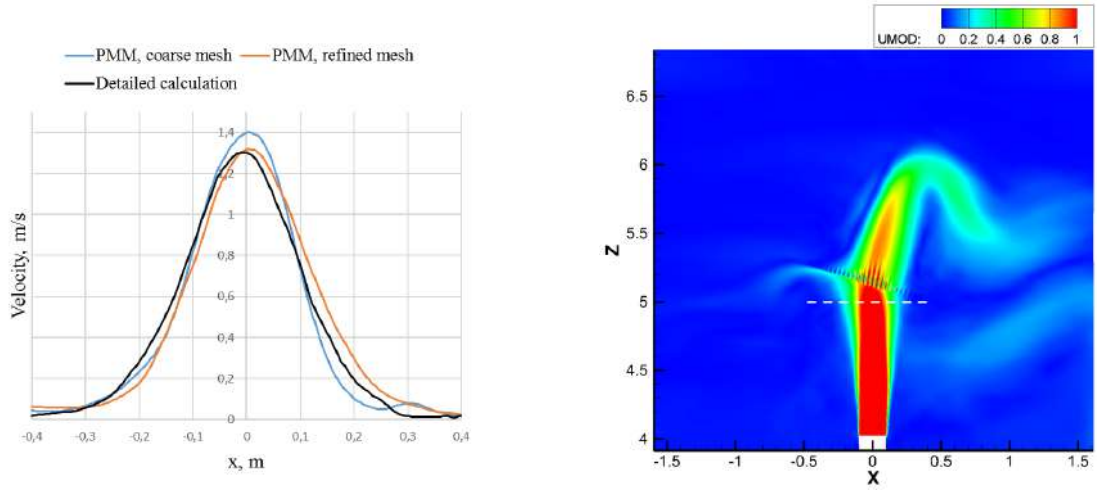

(a) (b)

Figure 10. Distribution of the velocity magnitude (a) in the jet before the obstacle (b)

Figure 11a shows the comparison of the time-averaged velocity magnitude values in a coordinate system tied to the inclined grid ($x1 = x \cdot \cos(17°) - z \cdot \sin(17°)$, $z1 = x \cdot \sin(17°) + z \cdot \cos(17°)$), along a line parallel to the inclined grid at a distance of 10 cm from it (Fig. 11b) in the detailed calculation and in the calculations using PMM. The hydrodynamic loss coefficient of the flow in $z1$ direction, perpendicular to the grid, K_{loss} was adjusted using a series of calculations to achieve the best match with the detailed calculation results for the same averaging time interval ($K_{loss} = 35m^{-1}$ in the coarse mesh, $K_{loss} = 20m^{-1}$ in the refined mesh).

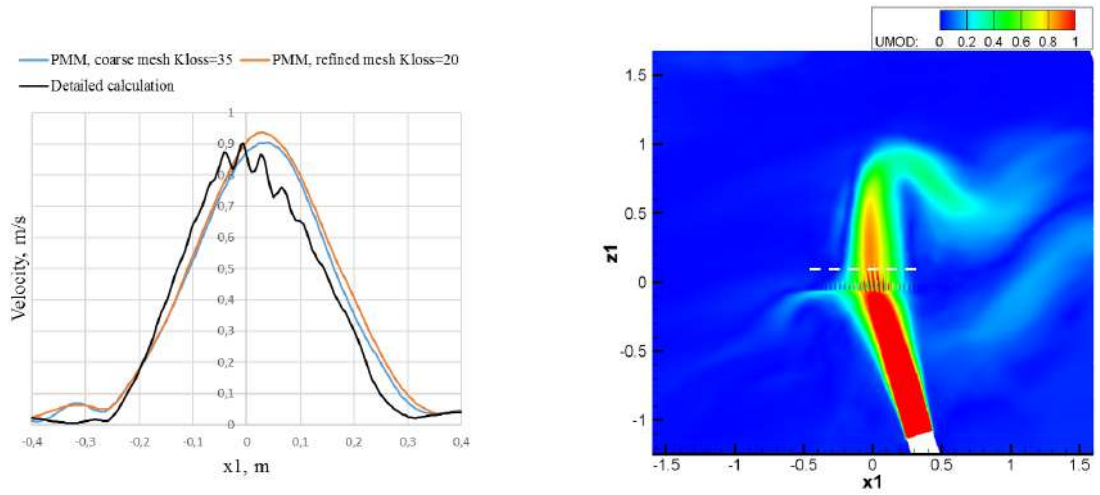

(a) (b)

Figure 11. Distribution of the velocity magnitude (a) in the flow above the inclined grid (b)

The maximum velocity drop in the flow passing through the inclined grid in the detailed calculation is 29.58%; the maximum velocity drop in the flow passing through the PMM area is 36.79% for the coarse mesh and 30.38% for the refined mesh.

The calculation results of H2P1_10 test with the CABARET-SC1 code using the porous medium model with the adjusted hydrodynamic loss coefficient $K_{loss} = 20m^{-1}$ in the refined mesh led to a good agreement in the evolution of the helium-rich layer erosion and the temperature distribution with the experimental data (Figs. 12–14).

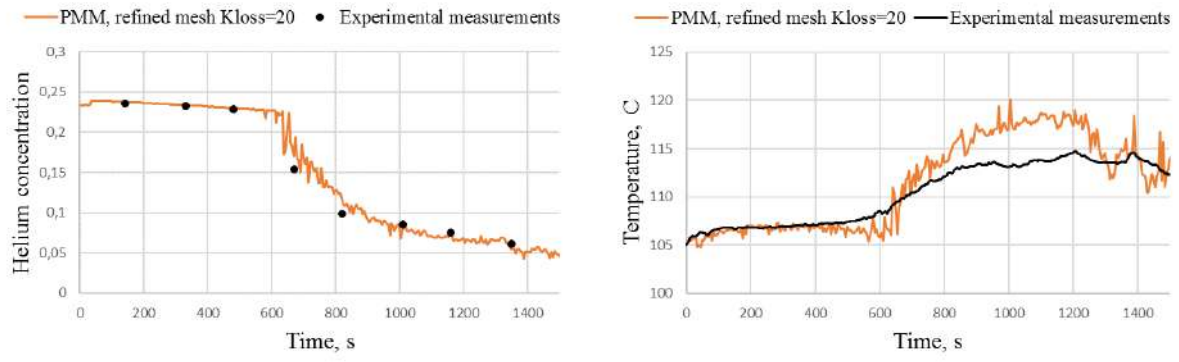

(a) (b)

Figure 12. Comparison of the evolution of calculated helium concentration (a) and temperature (b) with the experimental measurements at 2926 mm above the steam injection level

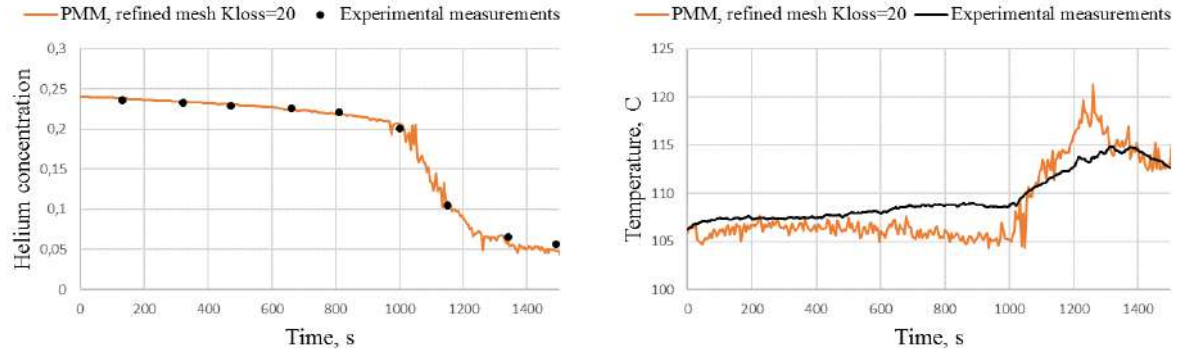

(a) (b)

Figure 13. Comparison of the evolution of calculated helium concentration (a) and temperature (b) with the experimental measurements at 3478 mm above the steam injection level

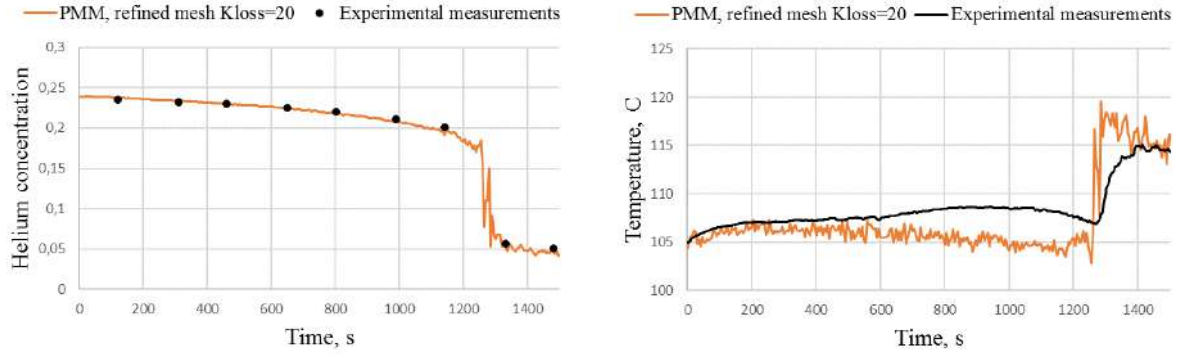

(a) (b)

Figure 14. Comparison of the evolution of calculated helium concentration (a) and temperature (b) with the experimental measurements at 4030 mm above the steam injection level

In the developed porous medium model, heat losses on the grid were not modeled. This causes the temperature of the steam after passing through the grid and then in the area of contact with the helium-rich layer to be overestimated. Also, after passing through the PMM, the flow velocity oscillations are almost nullified. Figures 15 and 16 show a qualitative comparison of the TKE distribution in the detailed calculation, PMM calculation and the experiment. The TKE value is determined as:

$$TKE = \frac{1}{2}\left((\sigma V_x)^2 + (\sigma V_z)^2 + \frac{1}{2}\left[(\sigma V_x)^2 + (\sigma V_z)^2\right]\right),$$

where σV_x and σV_z are the standard deviations of the velocity components in $y = 0$ plane. In the experiment, two-dimensional velocity fields in the rectangular area above the grid (the field of view) were recorded using the PIV (Particle Image Velocimetry) system during several time periods.

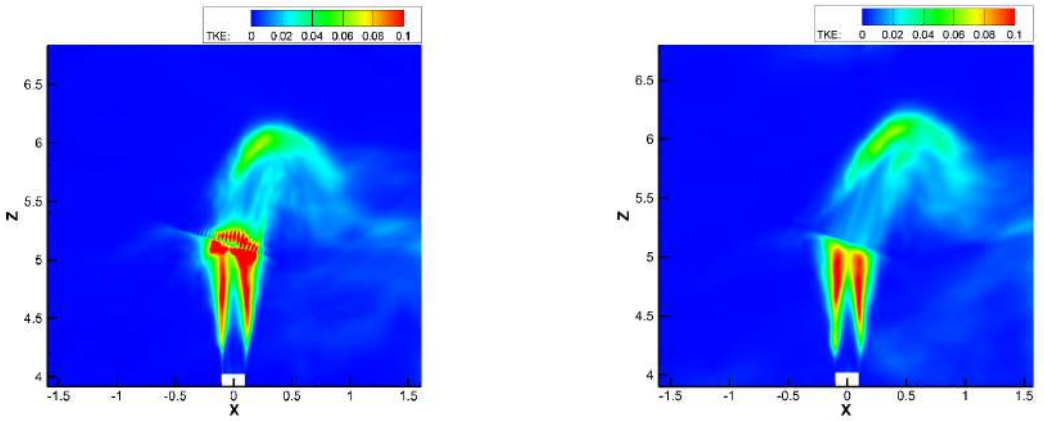

(a) Detailed calculation averaged over 40–70 s (b) PMM refined grid $K_{loss} = 20m^{-1}$ averaged over 40–70 s

Figure 15. Calculated TKE distributions

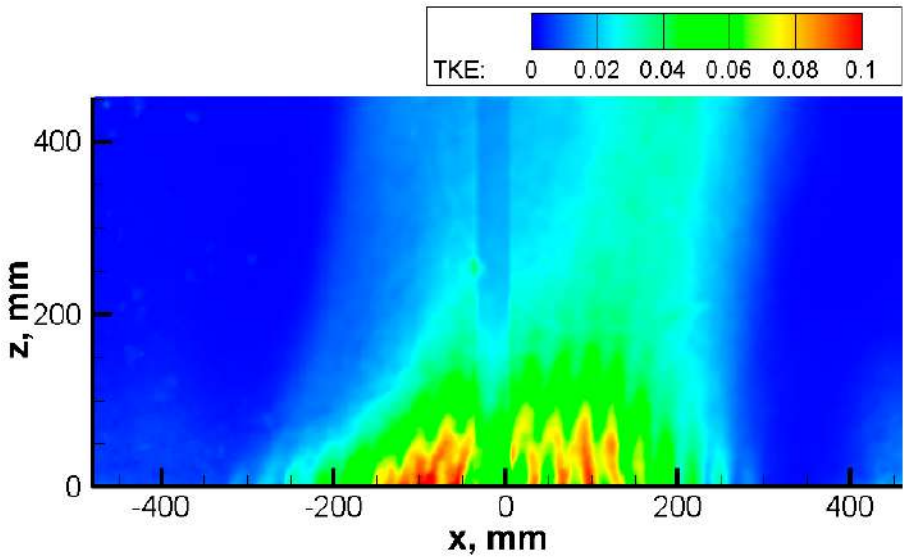

Figure 16. TKE distribution in the PIV field of view. Measurements were recorded over a time period of 743.6–948.4 s

Due to the absence of velocity oscillations behind the grid, the deflected flow mixes with surrounding atmosphere less intensively and its velocity in the area of contact with the helium-rich layer is overestimated. One of the OECD/NEA HYMERES project participants conducted H2P1_10 test simulation in the RANS approximation [8] also using PMM. Taking into account heat losses on the grid and with the adjusted velocity oscillation distribution behind the grid, the hydrodynamic loss coefficient of the flow in the direction perpendicular to the inclined grid was estimated as $K_{loss} = 15m^{-1}$.

Conclusion

The experiments conducted in the OECD/NEA HYMERES project covered a wide range of complex interconnected processes and phenomena. The most comprehensive understanding of the physical phenomena observed in experiments. The calculations of complex flows with obstacles in the OECD/NEA HYMERES benchmark tests with the CABARET-SC1 CFD code showed that insufficient local resolution of vortex structures can affect the simulated transient differently. In the HP1_6_2 benchmark test simulations, the resolution of the mesh in the jet area significantly affects the flow pattern behind the obstacle in the path of the jet. Insufficient mesh resolution leads to an underestimation of the helium-rich layer dissolution dynamics. In the H2P1_10 benchmark test simulations insufficient mesh resolution in the jet area, on the contrary, leads to an overestimation of the time required for complete mixing of the helium layer. The absence of other tuning parameters in the numerical approach allows evaluating the influence of separate physical processes on the observed experimental picture. Inclusion of the radiation heat transfer model in the computational model led to a good agreement with experimental measurements for both temperature and the dynamics of the helium-rich layer mixing.

The calculation of the H2P1_10 test was conducted using a porous medium model (PMM) simulating the resistance of a metal grid to the jet flow. The hydrodynamic loss coefficient in the PMM was adjusted using the results of a detailed calculation (with the direct mesh resolution of the steam flowing through the grid). This approach allowed achieving good agreement of the calculation results using the porous medium model with experimental measurements.

Acknowledgements

This research uses the data from the high quality experiments conducted in PSI in the framework of HYMERES project. We thank our colleagues from HYMERES-1 and HYMERES-2 groups who provided insight and expertise that greatly assisted the research.

The research is carried out using the equipment of the shared research facilities of HPC computing resources at Lomonosov Moscow State University [13].

References

1. Afanasiev, N., Goloviznin, V., Solovjev, A.: CABARET scheme with improved dispersion properties for systems of linear hyperbolic-type differential equations. Numerical Methods

and Programming 22, 67–76 (2021). https://doi.org/10.26089/NumMet.v22r105

2. Andreani, M., Gaikwad, A.J., Ganju, S., *et al.*: Synthesis of a CFD benchmark exercise based on a test in the PANDA facility addressing the stratification erosion by a vertical jet in presence of a flow obstruction. Nuclear Engineering and Design 354, 110177 (2019). https://doi.org/10.1016/j.nucengdes.2019.110177

3. Bal, R.S.: Nuclear Safety in Light Water Reactors. Elsevier, 2012. https://doi.org/10.1016/C2010-0-67817-5

4. Bolshov, L., Glotov, V., Goloviznin, V., *et al.*: Cabaret-Sc1 Code Validation in Experiments on Hydrogen Explosion Safety at NPP. Atomic Energy 127, 216–222 (2020). https://doi.org/10.1007/s10512-020-00613-7

5. Filippov, A., Grigoryev, S., Tarasov, O.: On the possible role of thermal radiation in containment thermal-hydraulics experiments by the example of CFD analysis of TOSQAN T114 air-He test. Nuclear Engineering and Design 310, 175–186 (2016). https://doi.org/10.1016/j.nucengdes.2016.10.003

6. Jammal R., *et al.*: The Fukushima Daiichi Accident. IAEA, Vienna, Austria (2015).

7. Kanaev, A.: Modeling of the influence of local heat sources on a light gas stratification formation and erosion in a large-scale experimental facility using eddy resolving numerical approach. Nuclear Engineering and Design 421, 113037 (2024). https://doi.org/10.1007/s10512-020-00613-7

8. Kelm, S., Liu, X., Liu, X., *et al.*: The Tailored CFD Package 'containmentFOAM' for Analysis of Containment Atmosphere Mixing, H2/CO Mitigation and Aerosol Transport. Fluids 6(3), 100 (2021). https://doi.org/10.3390/fluids6030100

9. Paladino, D., Mignot, G., Kapulla, R., *et al.*: OECD/NEA HYMERES Project: For the Analysis and Mitigation of a Severe Accident Leading to Hydrogen Release Into a Nuclear Plant Containment - 14322. American Nuclear Society, United States. https://www.oecdnea.org/jointproj/hymeres.html

10. Paladino, D., Kapulla, R., Paranjape, S., *et al.*: PANDA experiments within the OECD/NEA HYMERES-2 project on containment hydrogen distribution, thermal radiation and suppression pool phenomena, Nuclear Engineering and Design 392, 111777 (2022). https://doi.org/10.1016/j.nucengdes.2022.111777

11. Paranjape, S., *et. al.*: OECD-NEA/HYMERES project: PANDA Test HP1_6_2 Quick-Look Report. Tech. Rep. TM-42-15-08, Rev-0, HYMERES-P-15-20 Paul Scherrer Institute (2015).

12. Paranjape, S., *et. al.*: OECD-NEA/HYMERES project: PANDA test facility description and geometrical specifications. Tech. Rep. TM-42-13-12, HYMERES-P-13-04 Paul Scherrer Institute (2013).

13. Voevodin, Vl., Antonov, A., Nikitenko, D., *et al.*: Supercomputer Lomonosov-2: Large Scale, Deep Monitoring and Fine Analytics for the User Community. In Journal: Supercomputing Frontiers and Innovations 6(2), 4–11 (2019). https://doi.org/10.14529/jsfi190201